ADAPTIVE RESONANCE THEORY APPLIED TO MOSA MONITORING

G. R. S. Lira*, E. G. Costa, V. S. Brito, A. C. Silva and L. A. M. Martins.

Federal University of Campina Grande, Brazil.
*Email: george@dee.ufcg.edu.br

Abstract: A monitoring and diagnosis technique for metal oxide surge arrester (MOSA) is proposed in this study using a neural network scheme known as Adaptive Resonance Theory (ART), which forms clusters of data and is trained without a supervisor. It can achieve the self-organization of input codes for pattern classification in response to random sequences of input patterns. The input patterns considered in this work are the thermal profiles of the MOSA when in normal operation (i.e. submitted to system voltage). Several tests were carried out using faulty and non-faulty MOSAs. The most common failures in MOSA were simulated in laboratory: sealing problems, internal humidity, varistor degradation and superficial pollution. The thermal profiles obtained from these tests were employed in the ART training and test. Good results were obtained in the tests that were carried out. Hit ratios greater than 98% were achieved. Therefore, this technique may be used as a tool at electrical utilities in their activities of monitoring and predictive maintenance.

1 INTRODUCTION

Metal oxide (ZnO) surge arresters (MOSA) are equipments applied to power system protection against several kinds of surges. During the occurrence of lightning or switching surges, a voltage higher than the equipment insulation level can be reached. If the surge arresters are working properly, they are able to limit overvoltages, avoiding damages to the protected equipment. A defective arrester may not be able to provide the proper protection level in substations, exposing the equipment and personnel to risk. Thus, MOSAs decisively contribute to an increase in reliability, economy and operation continuity of the systems which they protect. Therefore, the development and improvement of tools and techniques that might aid in the monitoring and diagnosis of failures in surge arresters is very important in order to guarantee adequate operation conditions.

Monitoring of surge arresters is usually conducted by means of leakage current measurement or thermal image inspections. But, among power companies, there is no standard procedure for the monitoring and analysis of the obtained results. Besides, when some abnormality is detected, the arrester is replaced by a new one and no further study is conducted to evaluate what kind of problem happened to it.

In this paper, the diagnosis by thermal images is approached. This technique is subjected to imprecision, since the diagnosis is based on pre-defined comparative parameters obtained empirically and in the specialist knowledge.

In order to overcome the limitations present in MOSA diagnosis by thermal images, a new monitoring and diagnosis technique for metal oxide surge arresters (MOSA) is proposed in this paper using a neural network scheme known as Adaptive Resonance Theory (ART), which forms clusters of data and is trained without a supervisor. The proposed diagnosis technique is based on analysis by the ART network from the thermal profile of the MOSA when in normal operation (i.e. submitted to the system voltage). From the MOSA thermal profile, the ART network can identify failures in the MOSA.

After some tests, high hit success ratios were obtained which encourage the employment of the technique as a useful tool at power system utilities in their predictive monitoring activities, as well as assisting in the manufacturing process of more robust surge arresters.

2 ZNO SURGE ARRESTERS

The ZnO surge arrester arises as an alternative to protect power systems against transient voltage surges, decreasing surge levels in transmission and high voltage equipments. Nowadays, this kind of arrester is being used more and more, due to its high energy absorption capability and highly nonlinear V-I characteristic that allows the arresters projects without gaps, which causes several mechanical problems and uncertainty in relation to the surge arrester performance.

2.1 Constructive aspects

ZnO surge arresters are equipments with simple structure. Basically, they are composed by a column of ZnO varistors involved by porcelain or a polymeric column. Its configuration depends on the application, but in general it presents the appearance shown in Figure 1, where the main elements are pointed out.

The major components of the arresters are the ZnO blocks – varistors. Its format is commonly cylindrical with diameter and height depending on the desired energy absorption capability and voltage level, respectively. The diameter varies from 30 mm for distribution systems up to 100 mm or more for high and extra-high voltage systems. The height varies from 20 mm up to 45 mm. It is limited by ZnO grains homogeneity resultant from the manufacturing process. The greater the varistor volume, the more difficult it is to guarantee the grains homogeneity [1].

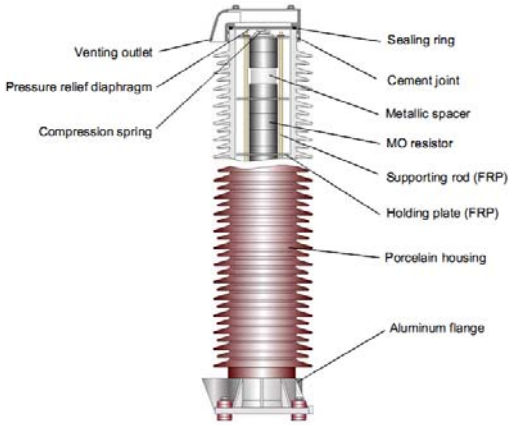

Figure 1: Basic structure of a porcelain housed ZnO surge arrester [1].

The ZnO block and the other internal components are involved by an insulating column of vitrified porcelain or polymeric material. These components intend to avoid the humidity infiltration and the accumulation of pollution in the surface. The columns hold sheds to provide an adequate creepage distance.

3 LABORATORY MEASUREMENTS

Operation voltage tests were carried out with nine different MOSAs aiming to obtain thermal images of surge arresters under failure and non-failure conditions. Seven arresters with 96 kV rated voltage, one with 192 kV and other with 550 kV were tested. The diagram of the test arrangement is shown in Figure 2. The surge arresters were submitted do Maximum Continuous Operating Voltage (MCOV) during the tests.

Before testing each surge arrester, an analysis was made of its status and electrical behavior before opening it, i.e., the status in which they came to the laboratory. The characteristic curve was analyzed, as well as thermal behavior and the status of the active column of varistors. Herewith, it was possible to construct the database corresponding to the non-defective surge arresters.

To obtain the thermal images corresponding to the defective surge arresters, several kinds of failures were artificially inserted into the evaluated MOSAs.

In a general sense, when some equipment was obtained for analysis, after its retrieval from the power system, or when degradation and aging tests were performed in the arresters, there were a series of defects more frequently found: sealing loss, varistor degradation, external pollution, internal humidity, the varistor displacement along the active column and non-uniform voltage distribution.

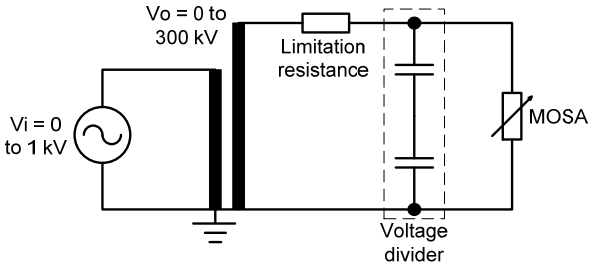

Figure 2: Diagram of laboratory test arrangement.

Following this, the defects simulated in laboratory in the evaluated surge arresters are described:

- **Sealing loss:** is characterized by the loss of physical isolation between environment and the interior of the surge arrester, allowing the exchange of gases. The loss of isolation yields to changes in warming characteristics of the arrester due to the gas circulation. The sealing loss was created artificially in laboratory by opening communication channels between the environment and the interior of the arrester, allowing the gases to exit and exchange heat.

- **Internal humidity:** can occur in surge arresters due to failures in the manufacturing process at the moment of the sealing, or by the sealing loss caused by the natural aging process of the equipment. The major problem raised by the internal humidity is the occurrence of partial discharge caused by the formation of water vapor in the arrester interior. To simulate this defect, the arresters were open and water was aspersed in the varistor column. Then, the arrester was closed.

- **Superficial pollution:** can produce the appearance of dry bands on the porcelain surface. These dry bands yield to superficial discharges in the porcelain, changing the electrical field in the region and causing varistor heating located at the same height of the column where the dry bands are formed. The presence of superficial pollution in the porcelain is a very common reason of failures or heating in surge arresters. To simulate this defect, salt moisture was aspersed on the entire porcelain of the surge arrester.

- **Varistor degradation:** can occur due to natural aging, precocious aging or varistor break. The precocious degradation is a factor that can contribute to the process of thermal avalanche in the surge arrester and so, the varistors break or explode and, consequentially, definitively damage the equipment. To simulate this failure in laboratory, damaged varistors were inserted in the arrester active column. The varistors were damaged by electrical stress produced by the application of current impulses and overvoltages at the varistors.

- **Displacement along the active column:** generally occurs due to inadequate transportation or storage of the surge arresters. However, this kind of problem may be caused by the manufacturing process due to assembly errors. The displacement causes the creation of preferential conductive ways in the region of the best contact, which produces an overheating in the region and a premature degradation of the varistors. In the simulation, displacements at active column were performed.

- **Non-uniform voltage distribution:** occurs due to failures in the arrester project or superficial pollution on the arresters. It originates electrical field concentration in the region close to the high voltage terminal or in the more polluted areas, which conduct premature degradation of varistors. In the simulation of this kind failure, several assemblies were used with and without equalizer rings.

In Figures 3(a) and 3(b) two thermal images of surge arresters are shown. The first one corresponds to a non-defective arrester, since there are not high temperature gradients in the arrester submitted to operation voltage. In the other thermal image, high temperature gradients were observed, so it was concluded that the arrester has some kind of problem.

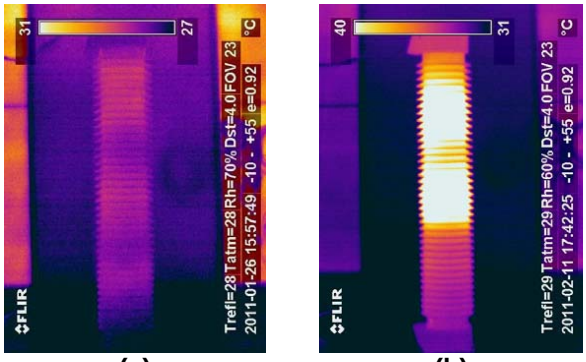

(a) **(b)**

Figure 3: Thermal images of: (a) non-defective MOSA and (b) defective MOSA.

4 ARTIFICIAL NEURAL NETWORKS

Artificial Neural Networks (ANN) are networks inspired by the brain structure, aiming to obtain characteristics similar to the human behavior, such as: learning, association, generalization and abstraction [2], [3]. The ANN can generalize the results obtained for data previously unknown, i.e., providing consistent answers for standards or examples not used in their training [2].

The major characteristics of ANN are: (i) learning capability, (ii) generalization capability, (iii) adaptation capability, (iv) error tolerance and (v) distributed computation. Such as the human brain, the organization of the artificial neurons connected by synaptic links (mathematical functions) is used to store and provide knowledge.

4.1 ART networks

The Adaptive Resonance Theory (ART) [4] network is a system that organizes input patterns in recognition classes, keeping the balance between the plasticity (discrimination) and stability (generalization) proprieties. Plasticity is the ability of a network to adapt and learn a new pattern well at any stage of operation, i.e., the network can create new pattern classes when an unfamiliar pattern stimulates the system [5]. Stability is the ability of grouping similar patterns in the same recognition class/cluster. The ART network provides a mechanism by which the network can learn new patterns without forgetting (or degrading/corrupting) old knowledge. So, it attempts to overcome the stability-plasticity dilemma.

Usually, an ART network has two complementary subsystems, which interact between themselves in the input pattern processing [5]:

- Attention subsystem: consists of two layers of neurons (comparison and recognition) with feed-forward and feed-backward characteristics. This system determines whether the input pattern matches one of the prototypes stored. When a match occurs the resonance is established.

- Orientation subsystem: deals with mismatch input patterns, inhibiting the attention subsystem with regard to these inputs.

There are several kinds of ART models/networks: ART1 [6], ART 2 [7], ART 3 [8], ARTMAP [9], Fuzzy ART [10], Fuzzy ARTMAP [11], Simplified Fuzzy ARTMAP [12, 13], among others.

The traditional ART model implementation is quite intricate due to its complex architecture and algorithms. However, some researchers have

simplified the traditional ART models [12, 13] aiming to ease the utilization of this kind of network. In this paper, the Simplified Fuzzy ARTMAP (SFAM) [12] model was employed in the MOSA diagnosis, because SFAM has reduced computational overhead and architectural redundancy. Also, this model employs simply learned equations with a single user-selectable parameter and one can learn every single training pattern with only a few training iterations [14].

4.2.1 Simplified Fuzzy ARTMAP (SFAM) The SFAM network is based on Fuzzy ARTMAP (FAM) [11] network. Basically, SFAM is a two layer net containing an input and an output layer, which employs a supervised training mode for pattern classification problems [14].

The main idea of SFAM is as follows [13]:

- Find the nearest subclass prototype that 'resonates' with the input pattern (winner).
- If the labels of the subclass and the input pattern match, update the prototype to be closer to the input pattern.
- Otherwise, reset the winner, temporarily increase the resonance threshold (*r*), and try the next winner.
- If the winner is uncommitted, create a new subclass (assign the input vector to the prototype pattern of the winner, and label it as the class label of the input).

The input of the network (**I**) is formed by the union of the raw input pattern ($\mathbf{a} \in \Re^M$) and its complement coder version ($\mathbf{a}^c = \mathbf{1} - \mathbf{a}$ for $\mathbf{a} \subset [0,1]$). The complement coded input then flows into the input layer and remains there. Weights (*w*) from each of the output category nodes flow down to the input layer. The category layer merely holds the names of the *N* number of categories that the network has to learn. Vigilance parameter and match tracking are mechanisms of the network architecture which are primarily employed for network training.

ρ is the vigilance parameter which can range from 0 to 1. It controls the granularity of the output node encoding. Thus, while high vigilance values make the output node much fussier during pattern encoding, low vigilance renders the output node to be liberal during the encoding of patterns.

The match tracking mechanism of the network is responsible for the adjustment of vigilance values. Thus, an error occurs in the training phase during the classification of patterns.

The SFAM algorithm is as follows [13]:

1) Set the vigilance factor equal to its baseline value:

$$\rho = \overline{\rho} \tag{1}$$

2) Insert input, and calculate second layer activities (T_j):

$$T_j(\mathbf{I}) = \left|\mathbf{I} \wedge \mathbf{w}_j\right| \Big/ \left(\alpha + \left|\mathbf{w}_j\right|\right) \tag{2}$$

where α is between 0.01 and 10, $\wedge$ is the fuzzy AND operator and for the uncommitted neuron: $T_N = T_0$;

3) Find the winner:

$$J = \arg\left[\max_j (Tj)\right] \tag{3}$$

If the winner neuron is uncommitted, go to step 7;

4) Check the resonance condition, i.e. if the input is similar enough to the winner's prototype:

$$\left|\mathbf{I} \wedge \mathbf{w}_j\right| \Big/ \left|\mathbf{I}\right| = \left|\mathbf{I} \wedge \mathbf{w}_j\right| \Big/ M \geq \rho \tag{4}$$

If this condition is fulfilled, go to step 5. If this condition is not fulfilled, reset the winner (T_j = -1) go to the step 3, and check the next winner

5) If the class label of the winner matches the class label of input, update the prototype pattern to be closer to the input pattern:

$$\mathbf{w}_J^{(new)} = \beta(\mathbf{I} \wedge \mathbf{w}_J^{(old)}) + (1-\beta)\mathbf{w}_J^{(old)} \tag{5}$$

and go to step 9, otherwise reset the winner (T_j = -1), temporarily increase the vigilance factor so as to violate the condition of (4), i.e. set ρ equal to:

$$\rho = \left|\mathbf{I} \wedge \mathbf{w}_j\right| \Big/ M + \varepsilon, \tag{6}$$

where ε is a small positive number, i.e. $\varepsilon \approx$ 0.001 and β in (5) is the learning factor ($0 \leq \beta \leq 1$);

6) If ρ > 1, terminate the training for this input pattern in the current epoch (data mismatch), and go to step 9, otherwise go to step 3, and try the next winner.

7) Create a new subclass, i.e. assign the input vector as the prototype pattern of the winner neuron:

$$\mathbf{w}_N = \mathbf{I}, \tag{7}$$

and set the class label of the winner neuron to be as the class label of input pattern.

8) Create a new uncommitted neuron, and: $N \leftarrow N+1$.

9) Go to step 1, and repeat the Algorithm for the next input.

5 PROPOSED METHODOLOGY

The proposed methodology is divided into three phases. The first one consists of the pre-processing phase, where the thermal profile database is built. This database will be used in the second and third phases of the methodology, which are the training and testing of SFAM network. The training process allows the employment of SFAM as a classifier, able to distinguish defective and non-defective surge arresters from their thermal profiles. In the testing process, the correct classification rate of the network is estimated.

- **Phase 1:** *The pre-processing phase* - In the pre-processing phase, the MOSA thermal images acquired in the laboratory tests were processed and joined to form a thermal profile database. For each thermal image, the temperature points along the porcelain housing were measured and stored, yielding a temperature vector of 200 points. Then, the temperature vectors were normalized to guarantee that the input patterns were between 0 and 1. The collection of these normalized temperature vectors result in the thermal profile database, which is formed, in this case, by 399 thermal patterns. In Figure 5 the typical thermal profile (not normalized) of defective surge arrester is shown.

- The profile shown in Figure 5 represents the desired result from a thermal image of a defective arrester well. It presents regions with more heating and less heating. The regions with more heating correspond to regions with varistors concentration. The oscillations in the profile are related to sheds of the porcelain. Higher temperatures are obtained in the porcelain re-entrances, which are closest to the varistors.

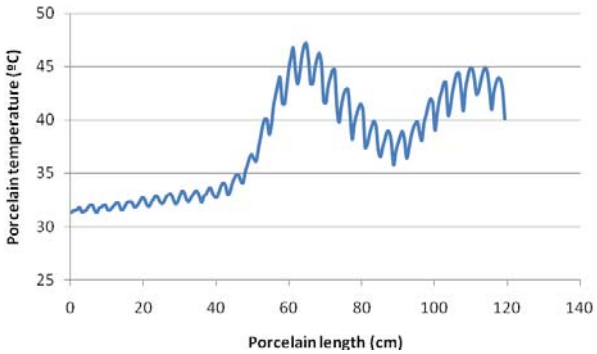

Figure 4: A typical thermal profile of a defective arrester.

- **Phase 2:** *SFAM network training* – In the training phase, a thermal profile database with 255 patterns randomly chosen from the original database was used. Each pattern in the database consists of a raw data on training process. During the training, the network tries to match the input pattern with its pre-defined category (employing the algorithm shown in the previous section); if no match occurs a new category is created. After the training, the network is able to classify the input patterns and determine if the pattern corresponds to a defective surge arrester or not.

- **Phase 3**: *SFAM network testing* – In this phase, a thermal profile database with 154 patterns randomly chosen from the original database and different of the training database was used to test the trained network, evaluating its adaptability and generalization proprieties, since just new patterns were shown in the network. So, the results yielded by the trained network for the test database were compared with the known/desired results. In this way, it was possible to estimate the Correct Classification Rate (CCR), which is defined by:

$$CCR = (c/t) \cdot 100, \tag{8}$$

where *c* is the number of correctly classified input data and *t* is the total number of data input.

6 RESULTS

The training and testing database were yielded to enable the diagnosis of the MOSA as defective or non-defective, so there are only two output categories in the databases. The following results were obtained from these network parameters: $\rho = 0.75$, $\alpha = 0.01$, $\beta = 1$, and 10 epochs.

After 100 random tests, an average CCR of 98.05%, average training and testing time of 4.17 s and 15.65 ms, were obtained respectively. The results show that more than 98% of the input patterns (154 were used on the tests), i.e, MOSA thermal profiles, were correctly classified as corresponding to defective or non-defective MOSA.

More laboratory measurements must be taken aiming to increase the training and testing database, allowing the identification of the failures on MOSA in the future. Likewise, new adjustments and improvements on the implemented classification must be performed. It is expected that these improvements will yield higher hit ratios and allow the identification of each kind of failure in surge arresters.

7 CONCLUSIONS

This paper proposed a diagnosis technique based on analysis, by the SFAM network, of the thermal profile of the MOSA, when in normal operation (i.e. submitted to the system voltage). From the MOSA thermal profile, the SFAM network could identify failures in the MOSA.

The obtained results confirm the efficiency of the artificial neural networks in the data classification. In the analyzed problem, 98.05% of input data was correctly classified as defective or non-defective. These results are encouraging, since the historical of the arresters and the experience of the maintenance engineering must be considered in the complete diagnosis.

To improve and to solidify the obtained results, it is possible to try to enrich the classification of thermal images in accordance with the kind of problem. However, the major difficultly found in the application of the proposed technique was the scarcity of data for the network training. Thus, more laboratory tests are necessary to increase the database for training and testing of the proposed diagnosis scheme.

8 REFERENCES

[1] V. Hinrichsen, “Metal-oxide surge arresters fundamentals,” 1st Edition. Siemens – Power Transmission and Distribution Power Voltage Division, Berlin, 2001.

[2] S. Haykin, Neural networks, A comprehensive Foundation. New York: Macmilan, 1994.

[3] A. Braga, A. Carvalho, and T. Ludermir, Redes Neurais Artificiais: Teoria e Aplicações. Rio de Janeiro: LTC, 2000.

[4] S. Grossberg, “Adaptive pattern classification and universal recoding, II: feedback, expectation, olfaction and illusions”, Biological Cybernetics, Vol. 23, pp. 187–202, 1976.

[5] A. S. Pandya and R. B. Macy, Pattern Recognition with Neural Networks in C++. USA: CRC Press, 1996.

[6] G. A. Carpenter and S. Grossberg, “A massively parallel architecture for a self-organizing neural pattern recognition machine”, Computer Vision, Graphics and Image Processing, vol. 37, pp. 54–115, 1987.

[7] G. A. Carpenter and S. Grossberg, “ART2: Self-organization of stable category recognition codes for analog input patterns”, Applied Optics, vol. 26, No. 23, pp. 4919– 4930, 1987.

[8] G. A. Carpenter and S. Grossberg, “ART3: Hierarchical search using chemical transmitters in self-organizing pattern recognition architecture, Neural Networks, Vol.3, pp. 129–152, 1990.

[9] G. A. Carpenter, G. S. Grossberg and J. H. Reynolds, “ARTMAP: Supervised real-time learning and classification of non-stationary data by a self-organizing neural network”, Neural Networks, Vol. 4, pp. 565–588, 1991.

[10] G. A. Carpenter, G. S. Grossberg and D. B. Rosen, “Fuzzy ART: Fast stable learning and categorization of analog patterns by an adaptive resonance system”, Neural Networks, Vol. 4, pp. 759–771, 1991.

[11] G. A. Carpenter, S. Grossberg, N. Markuzon, J. H. Reynolds, and D. B. Rosen, “Fuzzy ARTMAP: A neural network architecture for incremental supervised learning of analog multidimensional maps”, IEEE Trans. on Neural Networks, Vol.3, No. 5, pp. 698–713, 1992.

[12] T. Kasuba, “Simplified Fuzzy ARTMAP”, AI Expert, Vol. 8, No. 11, pp.18–25, 1993.

[13] M. Vakil-Gahimisheh and N. Pavešić, “A Fast Simplified Fuzzy ARTMAP Network”, Neural Processing Letters, Vol. 17, pp. 273–316, 2003.

[14] S. Rajasekaran, and G. A. Vijayalakshmi Pai, “Simplified Fuzzy ARTMAP as Pattern Recognizer”, Journal of Comput. in Civ. Eng., Vol.14, No. 2, pp. 92–99, 2000.